NJC

Accepted Manuscript

This article can be cited before page numbers have been issued, to do this please use: L. Biancalana, S. Fulignati, C. Antonetti, S. Zacchini, G. Provinciali, G. Pampaloni, A. M. Raspolli Galletti and F. Marchetti, *New J. Chem.*, 2018, DOI: 10.1039/C8NJ03569E.

ROYAL SOCIETY OF CHEMISTRY

rsc.li/njc

View Article Online
DOI: 10.1039/C8NJ03569E

Ruthenium *p*-Cymene Complexes with α-Diimine Ligands as Catalytic Precursors for the Transfer Hydrogenation of Ethyl Levulinate to γ-Valerolactone

Lorenzo Biancalana,[a,b] Sara Fulignati,[a,b] Claudia Antonetti,[a,b] Stefano Zacchini,[b,c] Giacomo Provinciali,[a] Guido Pampaloni,[a,b] Anna Maria Raspolli Galletti [a,b,*] and Fabio Marchetti [a,b,*]

[a] *Dipartimento di Chimica e Chimica Industriale, Università di Pisa, Via G. Moruzzi 13, I-56124 Pisa, Italy.*

[b] *CIRCC, via Celso Ulpiani 27, I-70126 Bari, Italy.*

[c] *Dipartimento di Chimica Industriale "Toso Montanari", Università di Bologna, Viale Risorgimento 4, I-40136 Bologna, Italy.*

Corresponding Authors

*E-mail addresses: anna.maria.raspolli.galletti@unipi.it; fabio.marchetti1974@unipi.it.

View Article Online
DOI: 10.1039/C8NJ03569E

Abstract

The ruthenium compounds [(η^6-*p*-cymene)RuCl{κ^2*N*-(HCNR)$_2$}]NO_3 (R = 4-C_6H_4Me, [**1**]NO_3; 4-C_6H_4OH, [**2**]NO_3; C_6H_{11} = Cy, [**3**]NO_3; 4-$C_6H_{10}OH$, [**4**]NO_3; ^{t}Bu, [**5**]NO_3) were prepared in high yields from [(*p*-cymene)$RuCl_2$]$_2$, $AgNO_3$ and the appropriate α-diimine. Compounds [**2**]PF_6 and [**4**]PF_6 were obtained by straightforward reaction of [(η^6-*p*-cymene)RuCl$(MeCN)_{0.66}$]PF_6, [**6**]PF_6, with α-diimine, whereas [**4**]BPh_4 was afforded by metathesis between [**4**]NO_3 and $NaBPh_4$. All the ruthenium products were characterized by analytical methods, IR, NMR and UV-Vis spectroscopy; in addition, the structure of [**1**]NO_3 was ascertained by a X-ray diffraction study. Compounds [**1-4**]NO_3, [**4**]PF_6 and [**4**]BPh_4 were investigated as catalytic precursors in the transfer hydrogenation reaction of ethyl levulinate to γ-valerolactone in isopropanol solution, under microwave irradiation. [**4**]BPh_4 revealed to be the best catalytic precursor, affording γ-valerolactone in 62% yield under optimized experimental conditions.

Keywords: biomass transformation, γ-valerolactone, ethyl levulinate, ruthenium arene complexes, α-diimine ligand, transfer hydrogenation

Introduction

Nowadays, the continuous depletion of fossil resources and the impact of environmental pollution due to carbon emission make necessary the search for renewable resources [1]. Biomass is an attracting alternative feedstock, being abundant, widespread, cheap and useful to produce valuable chemicals. In particular, γ-valerolactone (GVL) can be accessed from lignocellulosic biomass through hydrogenation of levulinic acid (LA) and related esters (including ethyl levulinate, EL, Scheme 1) [2], and it possesses notable properties (high boiling and flash points, low melting point and low vapor pressure) which make it a safe compound for industrial application and have spread its use over a range of applications, i.e. as a green solvent, biofuel, and sustainable starting material to obtain a variety of derivatives [2b,e,h,3].

View Article Online
DOI: 10.1039/C8NJ03569E

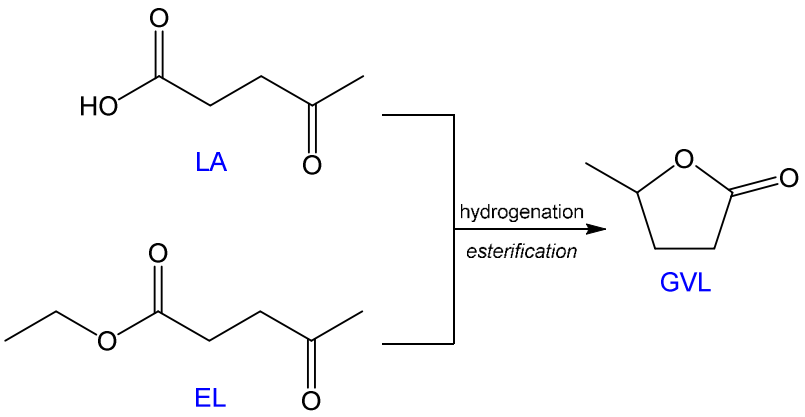

Scheme 1. Structures of levulinic acid (LA), ethyl levulinate (EL) and γ-valerolactone (GVL).

The hydrogenation process of LA or its esters, such as EL, to GVL has aroused a considerable attention on both academic and industrial level. Respect to LA, EL is attracting increasing interest since it can be directly synthesized in high yields from raw biomasses working in ethanol. This approach, due to its low cost and simple technology, is in alignment with the current tendency to sustain the development of green chemistry industry, highlighting the possibility of biomass utilization for the one-pot synthesis of EL. Moreover, unlike LA, EL possesses relatively low boiling point, easy recovery and acid-free characteristics, all properties that make this compound an attractive substrate for the synthesis of GVL [4].

The hydrogenation of LA and its esters to GVL has been carried out employing different hydrogen sources: molecular hydrogen [2h-j,2l,5], formic acid [5a,6] and alcohols [5a,7]. Recently, these two last alternative hydrogen sources are attracting great attention because they allow the conduction of the reaction under more safety and economic reaction conditions, due to the absence of molecular hydrogen as reactant. In fact, in these cases hydrogen can be generated *in situ* from the catalytic decomposition of formic acid [6a] or the reduction of the substrate can proceed through a catalytic transfer hydrogenation mechanism (TH) due to the interaction between an alcohol and the catalyst [7h,8]. This last method can be considered a green approach because the adopted alcohol acts both as solvent and hydrogen source.

View Article Online
DOI: 10.1039/C8NJ03569E

In this regard, in this work the TH of EL to GVL has been investigated using 2-propanol as the hydrogen source, due to the better performances of secondary alcohols than primary ones [7m]. Both heterogeneous and homogeneous catalysts have been reported in the literature for TH of LA and/or EL to GVL. The first ones are generally represented by supported precious metals [7j-m] and zirconium compounds [7e-h,n]. Regarding the homogeneous catalysts, the most important examples are the complexes of ruthenium [2c,5a,9] iridium [9a,10], palladium [11] and iron [5a,6b,7d]. Typically, homogeneous catalysts have high catalytic efficiency with, generally, high turnover numbers. However, up to now, only Dai et al. [7d] have investigated the synthesis of GVL from ethyl levulinate in alcoholic medium employing homogeneous catalysts. They tested a wide range of iron complexes and founded the best performances in the presence of iron(0)-cyclopentadienone-tricarbonyl system. The highest GVL yield reported by Dai et al., equal to 95%, was ascertained working with the catalyst amount of 1 mol% and the $NaHCO_3$ base amount of 5 mol%, both respect to the substrate, carrying out the reaction in 2-propanol at 100 °C for 19 hours starting from a 2 M ethyl levulinate solution. Despite the good GVL yield obtained by the authors, the reaction conditions present some drawbacks, such as the high amount of base and the very long reaction time. In this work, for the first time, arene ruthenium(II) complexes are investigated as catalytic precursors for the synthesis of GVL from EL through the TH approach, highlighting the potentiality of these complexes to be employed in an integrated bio-refinery approach. Ruthenium(II) arene complexes constitute a family of widely investigated compounds for their possible catalytic [12] and biological applications [13]. In particular, they have been intensively studied in the last decade as catalysts for hydrogenation reactions of ketones [14], following the breakthrough offered by the catalytic systems developed by Noyori [15], but not yet employed for TH of EL. Moreover, for the first time, microwave heating was employed in the TH of EL to GVL in the presence of homogeneous systems. In fact, up to now, microwaves have been employed only for the TH of LA in the presence of heterogeneous catalysts, such as Pd/C and Ru/C [7a,16] and for the TH of acetophenone with arene ruthenium(II) complexes [14e,17], proving that they are active also under

View Article Online
DOI: 10.1039/C8NJ03569E

microwave heating. It has to be remarked that the microwave treatment is a powerful tool favoring process efficiency, fast temperature increase, short reaction times and energy saving [18].

Results and discussion

1) Synthesis and characterization of Ru compounds.

α-Diimine ligands, (R)N=CHCH=N(R) (R = 4-C_6H_4Me, **L1**; 4-C_6H_4OH, **L2**; C_6H_{11} = Cy, **L3**; 4-$C_6H_{10}OH$, **L4**; ^{t}Bu, **L5**), were prepared by condensation of glyoxal with the appropriate primary amine, according to literature procedures (see Scheme 2a and Supporting Information) [19,20]. The unprecedented crystal structure of **L2** was ascertained by a X-ray diffraction study: an ORTEP view is shown in Figure 1, while relevant bonding parameters are given in Table 1. The molecular structure of **L2** resembles those previously reported for analogous α-diimine molecules, concerning the bonding parameters and the overall geometry [21]. Within the crystals, inter-molecular H-bonds are formed between the OH and N groups [O(1)-H(1A) 0.84 Å, H(1A)···N(1)#2 2.01 Å, O(1)···N(1)#2 2.8392(17) Å, <O(1)H(1A)N(1)#2 169.9 Å].

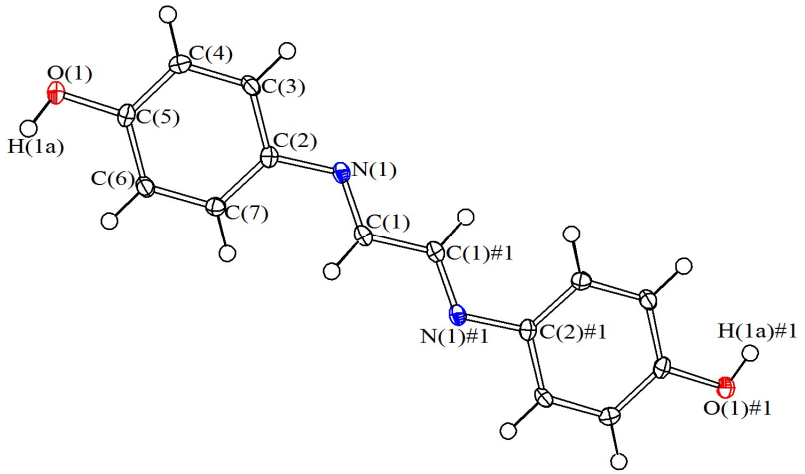

Figure 1. View of the structure of **L2**. Displacement ellipsoids are at the 50% probability level. Symmetry transformation used to generate equivalent atoms: #1 -x+2, -y+1, -z+1

Table 1.Selected bond distances (Å) and angles (°) for **L2**.

View Article Online
DOI: 10.1039/C8NJ03569E

C(1)−C(1)#1	1.450(3)	C(1)−N(1)	1.287(2)
C(2)−N(1)	1.4192(19)	C(5)−O(1)	1.3619(18)
N(1)−C(1)−C(1)#1	119.93(17)	C(1)−N(1)−C(2)	119.54(13)

Symmetry transformation used to generate equivalent atoms: #1 -x+2, -y+1, -z+1

The air stable ruthenium complexes [(η^6-*p*-cymene)RuCl{κ^2*N*-(HCNR)$_2$}]NO_3 (R = 4-C_6H_4Me, [**1**]NO_3; 4-C_6H_4OH, [**2**]NO_3; C_6H_{11} = Cy, [**3**]NO_3; 4-$C_6H_{10}OH$, [**4**]NO_3; ^{t}Bu, [**5**]NO_3) were synthesized upon treatment of [(*p*-cymene)$RuCl_2]_2$ with $AgNO_3$ in the appropriate solvent (acetonitrile or methanol) [22], followed by addition of the α-diimine **L1-L5** (Scheme 2b) [23]. Chloride abstraction is an essential step to obtain [**1-5**]NO_3, the direct interaction of [(*p*-cymene)$RuCl_2]_2$ with **L1**/**L3** otherwise leading to a mixture of different products (see SI for details). The synthesis of [**2-4**]NO_3 has been already reported [20], instead [**1**]NO_3 (90% yield) and [**5**]NO_3 (92% yield) are unprecedented.

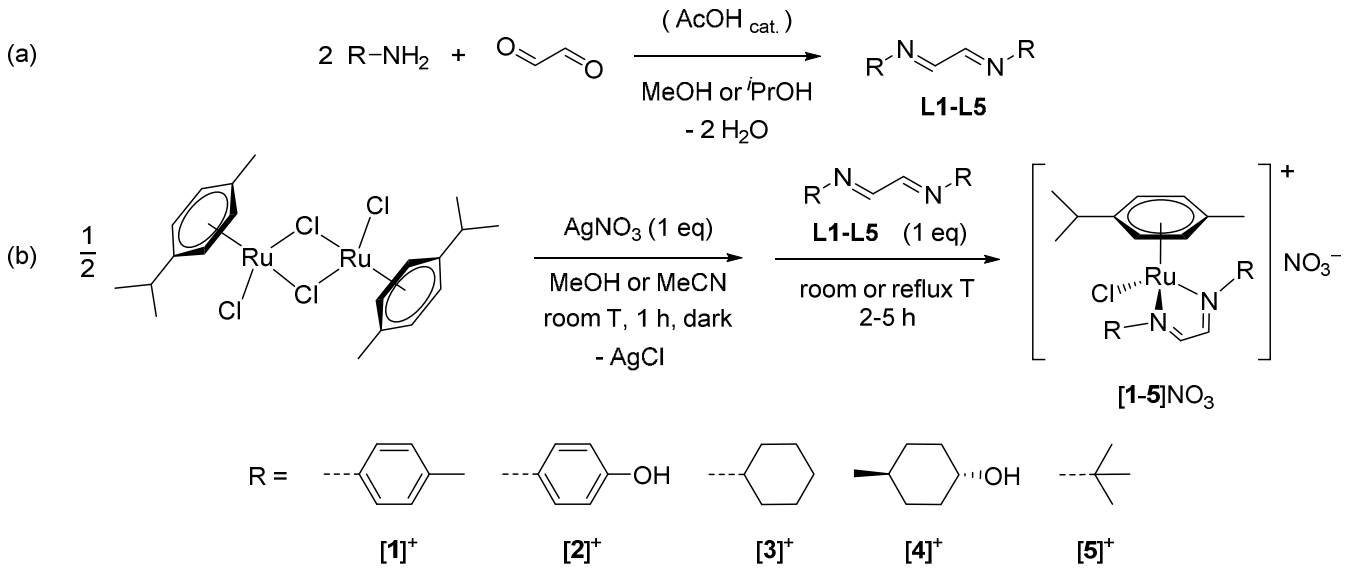

Scheme 2. Synthesis of α-diimine ligands **L1**-**L5** and related ruthenium complexes [**1**-**5**]NO_3.

The counterion is expected to play a fundamental role in the solution chemistry, and presumably in the catalytic behavior, of cationic Ru(II) arene complexes. In particular, it was previously demonstrated that

View Article Online
DOI: 10.1039/C8NJ03569E

the nature of the anion associated to [(arene)RuCl(α-diimine)]$^+$ [24] could be responsible for the formation of ion pairs and higher aggregates in organic solvents [24b,25].

On account of this feature, we synthesized new salts of the complexes [**2**]$^+$ and [**4**]$^+$, containing anions different from nitrate. In order to obtain [**2**]PF_6 and [**4**]PF_6, a two-step procedure similar to that used for the nitrate homologues (Scheme 2) was adopted. Thus, [(*p*-cymene)$RuCl_2$]$_2$ was allowed to react with NH_4PF_6 in acetonitrile, and the resulting solvato-species, [**6**]PF_6, was then isolated as an orange solid (Scheme 3a). This material did not correspond to the expected [(η^6-*p*-cymene)RuCl(MeCN)$_2$]PF_6 [26], but revealed to be a mixture of Ru compounds with overall MeCN/Cl and MeCN/*p*-cymene ratios = 0.66 (Cl analysis, ^{1}H NMR). Accordingly, [**6**]PF_6 is conveniently represented by the formula [(η^6-*p*-cymene)RuCl(MeCN)$_{0.66}$]PF_6. The use of CH_2Cl_2 in the work-up and the lability of the acetonitrile ligands [26c] may justify this result (see Experimental).

The reactions of [**6**]PF_6 with **L2** in MeOH at ambient temperature or with **L4** in refluxing MeCN afforded [**2**]PF_6 and [**4**]PF_6, respectively, in 80-90% yields (Scheme 3b).

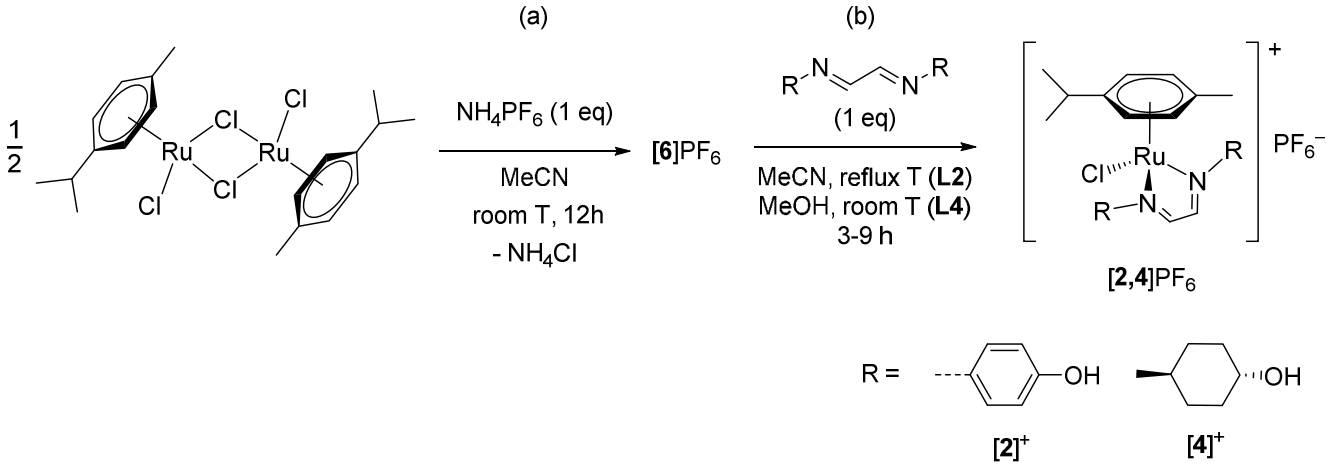

Scheme 3. Synthesis of ruthenium-α-diimine complexes [**2**-**4**]PF_6 via the acetonitrile intermediate [**6**]PF_6.

Compound [**4**]BPh_4 was obtained by anion metathesis between [**4**]NO_3 and $NaBPh_4$ in acetone at ambient temperature (eq. 1), and then isolated in 89% yield after work-up.

View Article Online
DOI: 10.1039/C8NJ03569E

$$[\mathbf{4}]NO_3 + NaBPh_4 \rightarrow [\mathbf{4}]BPh_4 + NaNO_3 \quad (1)$$

The novel ruthenium-α-diimine products were isolated as air-stable orange ([**4**]X, X = PF_6, BPh_4) or dark brown ([**1**]NO_3, [**2**]PF_6) crystalline materials, whereas hygroscopic orange-brown [**5**]NO_3 was stored under nitrogen. The complexes were characterized by analytical (CHN analysis, conductivity) and spectroscopic (NMR/IR/UV-Vis) methods. Selected data of all Ru compounds [**1-5**]X are compiled in Table S1, and compared to those of the related α-diimines **L1-L5**.

The solid-state IR spectra of [**1-5**]X (X = NO_3, PF_6) show strong absorptions due to the vibrations of the anion (*ca.* 1320 cm^{-1} and 830 cm^{-1} for NO_3^- and PF_6^-, respectively) and a medium/weak absorption in the 1530-1630 cm^{-1} region due to the anti-symmetric stretching of the N=CC=N moiety [27]. This band is substantially decreased in intensity, but not in wavenumber, on going from **L1**, **L2**, **L5** to the respective Ru complexes. Conversely, α-diimines with cyclohexyl rings (**L3**, **L4**) undergo a marked decrease in the wavenumber of the N=CC=N group upon coordination ($\Delta\nu = -85$ cm^{-1}). The UV-Vis spectra of [**1-5**]X (X = NO_3, PF_6, BPh_4) in CH_2Cl_2 or MeOH display MLCT bands around 270-280 and 420-450 nm [24a]. Enhanced intensity (ε) and additional absorption at *ca.* 550 nm were observed for [**1**]NO_3 and [**2**]X (X = NO_3, PF_6), comprising an extended π-system on the α-diimine.

In the NMR spectra, the HC=N unit within [**1-5**]$^+$ manifests itself with a ^{1}H signal at 8.3-8.7 ppm and a ^{13}C signal around 164-169 ppm, the latter being significantly deshielded ($\Delta\delta_C$ = 4-10 ppm) on coordination. The PF_6^- ion in [**2**]$^+$ and [**4**]$^+$ salts gives rise to a heptet at -145 ppm and a doublet around -70 ppm in the ^{31}P and ^{19}F spectra, respectively.

The ^{1}H NMR resonances of [**2**]PF_6 in DMSO-d_6 closely match those of the analogous nitrate salt, however a more evident line broadening can be observed for the latter even at high temperatures (60°C) [20]. This outcome can be explained on the basis of ion association phenomena [25,24b], which are significant in DMSO for [**2**]$^+\cdots NO_3^-$ but not for [**2**]$^+\cdots PF_6^-$. On the other hand, the ^{1}H NMR spectra of the *N*-cyclohexanol complex [**4**]$^+$ always feature sharp resonances, regardless of the solvent used

View Article Online
DOI: 10.1039/C8NJ03569E

(DMSO-d_6, CD_3OD or CD_2Cl_2) and the counter anion (NO_3^-, PF_6^- or BPh_4^-). Nevertheless, while ^1H spectra of [**4**]NO_3 and [**4**]PF_6 are almost identical in CD_3OD, the resonances of [**4**]BPh_4 are all considerably high-field shifted in this solvent, especially those related to the imine CH (7.63 ppm; $\Delta\delta_H$ = −0.70 ppm *vs.* NO_3^-/PF_6^- salts) and arene CH ($\Delta\delta_H \approx -0.15$ ppm) groups. In the case of [**5**]NO_3, the ^1H resonances due to the *p*-cymene ligand are broad at 25 °C in both $CDCl_3$ and D_2O solution, while being narrower on increasing temperature (up to 55 °C in $CDCl_3$). This behavior could be the consequence of hindered rotation of the *tert*-butyl groups, limiting the free rotation of the *p*-cymene ligand around the metal-centroid axis at 25 °C [28].

The solid state structure of [**1**]NO_3 was elucidated by single-crystal X-ray diffraction: an ORTEP view of the cation is shown in Figure 2, while relevant bonding parameters are given in Table 2. Complex $[\mathbf{1}]^+$ comprises the expected three-leg piano-stool geometry typical of other Ru(II)-arene compounds [29], and the bonding parameters around the Ru(II) centers are similar to those reported for [(*p*-cymene)RuCl(α-diimine)]$^+$ structures [20,24].

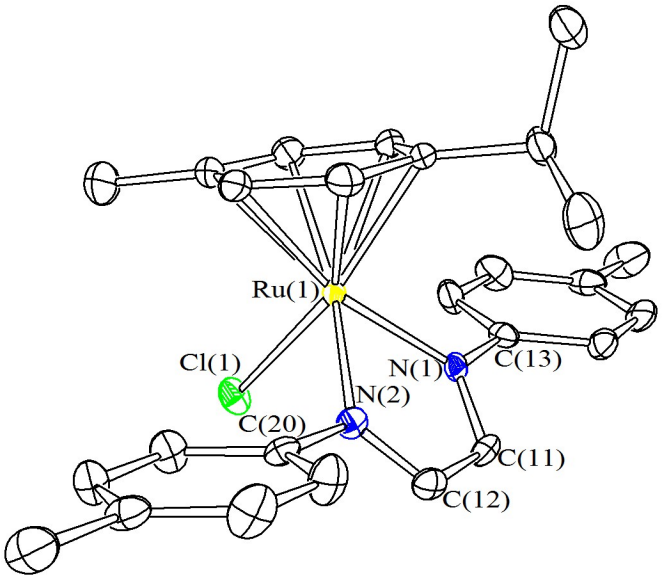

Figure 2. View of the structure of the cation $[\mathbf{1}]^+$ within **[1]NO_3**. Displacement ellipsoids are at the 50% probability level. Hydrogen atoms are omitted for clarity.

View Article Online
DOI: 10.1039/C8NJ03569E

Table 2. Selected bond distances (Å) and angles (°) for [**1**]$^+$.

Ru(1)-(η^6-p-cymene)$_{av}$	2.209(10)	Ru(1)−Cl(1)	2.3789(10)
Ru(1)−N(1)	2.065(3)	Ru(1)−N(2)	2.064(3)
N(1)−C(11)	1.288(5)	N(2)−C(12)	1.284(5)
N(1)−C(13)	1.428(5)	N(2)−C(20)	1.429(5)
C(11)−C(12)	1.436(6)		
N(1)−Ru(1)−N(2)	76.50(13)	Ru(1)−N(1)−C(11)	115.9(3)
N(1)−C(11)−C(12)	115.7(4)	C(11)−C(12)−N(2)	115.9(4)
C(12)−N(2)−Ru(1)	116.0(3)		

Compounds [**1**-**5**]X (X = NO_3, PF_6) are soluble in water; the solubility was assessed in saturated D_2O solutions at 21°C by ^{1}H NMR (Table S2). As expected, the presence of hydroxyl groups on the α-diimine ligand enhances water solubility (e.g., compare [**1**]NO_3 with [**2**]NO_3). However, the nature of the anion determines a more significant effect. Indeed, the solubility of [**2**]$^+$ and [**4**]$^+$ increases by 5-fold and 10-fold, respectively, on moving from the PF_6^- salt to the corresponding NO_3^- salt; instead [**4**]BPh_4 is almost insoluble in water, despite carrying OH groups on the α-diimine. Similarly, the substituents on the α-diimine and the anion strongly affect the solubility in organic solvents. Thus, [**2**]$^+$ and [**4**]$^+$, bearing hydroxyl groups on the α-diimine, are soluble as NO_3^- salts only in polar solvents (DMSO, water, alcohols), while [**1**,**3**,**5**]NO_3, lacking of OH groups, and also [**4**]BPh_4, are much better soluble in chlorinated solvents.

2) Catalytic study

The hydrogenation reactions of ethyl levulinate in isopropanol were carried out in a microwave reactor under magnetic stirring, and the resulting solutions were analyzed by gas chromatography. A first

View Article Online
DOI: 10.1039/C8NJ03569E

selection of Ru catalytic precursors included [**1**-**4**]NO_3, while [**5**]NO_3 was excluded due to its hygroscopicity.

It is generally assumed that the transfer hydrogenation reaction of ketones catalyzed by Ru(II) arene compounds proceeds through the intermediate formation of ruthenium-hydride species, initiating the catalytic cycle [30]. In general, a base activator is needed to achieve best performances, presumably allowing the conversion of the catalytic precursor into the active [Ru-H] form [31]. Nevertheless, some efficient catalytic systems have been reported, being able to generate the key hydride intermediate under base free conditions [32].

In the light of this preamble, in order to see whether in our case the use of a base was advantageous or not, preliminary reactions were carried out with [**3**]NO_3 as catalytic precursor, respectively in the presence and in the absence of 1 mol% NaOH (Figure 3) at 140 °C for 30 min.

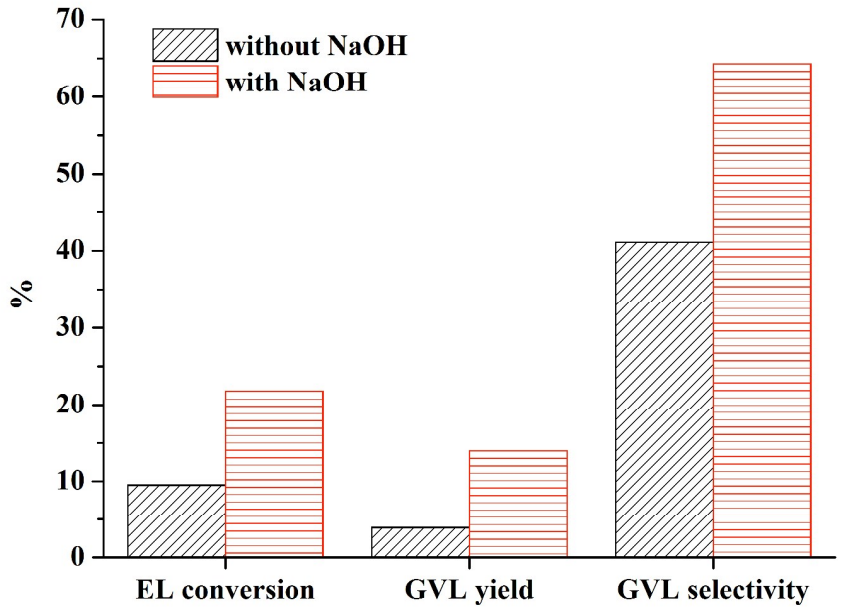

Figure 3. Effect of NaOH (1 mol% respect to EL) on ethyl levulinate (5 mmol) to γ-valerolactone conversion in 2-propanol (10 mL), using [**3**]NO_3 (0.1 mol% respect to EL) as catalytic precursor. MW heating, T = 140 °C, t = 30 min.

View Article Online
DOI: 10.1039/C8NJ03569E

The results indicate that NaOH supplies substantially higher conversion and selectivity (about 22% and 64%, respectively). Then, a screening was performed of the different ruthenium compounds as potential catalytic precursors, and the results are reported in Table 3.

Table 3. Catalytic performance of [**1-4**]NO_3 (0.1 mol% respect to EL) in the conversion of ethyl levulinate (EL, 5 mmol) to γ-valerolactone (GVL) in 2-propanol (10 mL). NaOH (1 mol% respect to EL); MW heating; T = 140 °C; t = 30 min. [a] 0.56 mol% respect to EL of catalytic precursor.

Run	Catalytic Precursor	EL conversion (%)	GVL selectivity (%)	GVL yield (%)
1	[**1**]NO_3	28.2	80.6	22.7
2	[**2**]NO_3	14.3	62.0	8.9
3	[**3**]NO_3	21.8	64.3	14.0
4	[**4**]NO_3	23.7	83.3	19.8
5 [a]	[**1**]NO_3	50.9	82.9	42.0
6 [a]	[**4**]NO_3	49.1	86.1	42.2

Compound [**2**]NO_3 exhibited the lowest activity and selectivity, and the activities obtained with the remaining catalytic precursors (runs 1, 3, 4 Table 4) under the same reaction conditions are similar, showing EL conversion in the range 22-28%. However, [**1**]NO_3 and [**4**]NO_3 appeared more promising than [**3**]NO_3, giving higher GVL selectivity (ca. 80%), and were thus selected for further studies.

First of all, due to the low activity ascertained for every complex, the amount of catalytic precursor was increased in order to increase EL conversion and the results reached employing an higher amount of complexes **[1]**NO_3 and **[4]**NO_3 are reported in runs 5 and 6 of Table 3, respectively. The increase of the catalytic precursor amount leads to an improvement of EL conversion, as expected, whereas GVL selectivity remains constant, allowing us to increase GVL yields, which are in both case double respect to the previous runs (runs 1 and 4, Table 1).

View Article Online
DOI: 10.1039/C8NJ03569E

Then, the effects of temperature and reaction time on the same catalytic precursors (**[1]**NO_3 and **[4]**NO_3**)** were then considered (Figure 4). Preliminary runs were carried out in order to establish the lowest temperature at which the catalytic precursors result active: negligible catalytic performances were observed at temperatures lower than 120°C. On this basis, the range 120-160°C was chosen in order to investigate the effect of temperature.

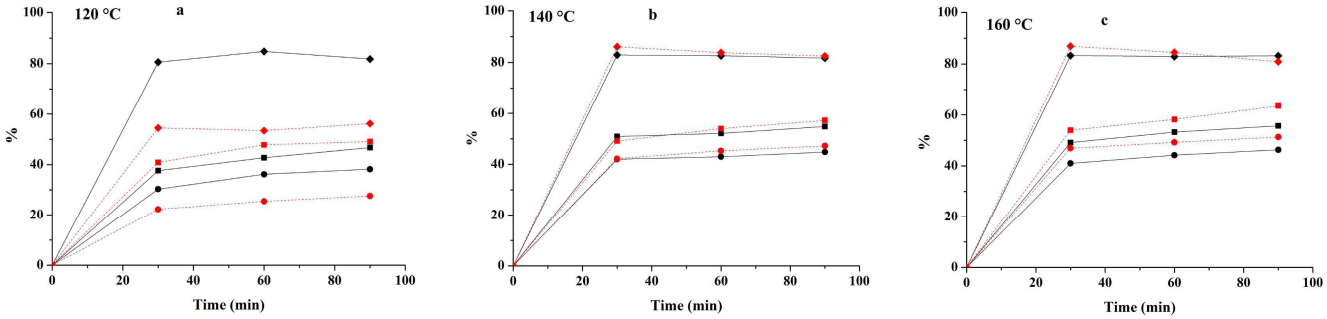

Figure 4. Profiles of EL (5 mmol) conversion (■■), GVL yield (●●) and GVL selectivity (♦♦) working with [**1**]NO_3 or [**4**]NO_3 (0.56 mol% respect to EL) in 2-propanol (10 mL), respectively; NaOH (1 mol% respect to EL); MW heating; T = a) 120 °C, b) 140 °C, c) 160 °C. Black solid line: compound [**1**]NO_3; red dashed line: compound [**4**]NO_3.

For both systems, prolonging the reaction over 30 minutes at fixed temperature scarcely affected the catalytic behavior. On the other hand, the catalytic performance strongly depends on the temperature. In fact, working at 120 °C, [**1**]NO_3 resulted more selective towards GVL than [**4**]NO_3, and afforded the highest GVL yield (Figure 4a). Probably, at low temperature the catalytic cycle is less favored employing [**4**]NO_3 than [**1**]NO_3 and in the presence of the first one EL can undergo side-reactions. When the temperature was increased to 140 °C (Figure 4b), the conversion values achieved with [**1**]NO_3 and [**4**]NO_3 after 30 minutes were higher than those at 120 °C (51% and 49% respect to 38% and 41%, respectively). Moreover, at 140 °C the selectivity with [**4**]NO_3 approached that given by [**1**]NO_3. When the temperature was further increased to 160 °C (Figure 4c), analogous selectivity to those ascertained at 140 °C were obtained for both complexes but an improvement of EL conversion was achieved with the

View Article Online
DOI: 10.1039/C8NJ03569E

system [**4**]NO_3 throughout the whole reaction time. In summary, raising the temperature revealed beneficial to the catalytic performance of [**4**]NO_3, allowing us to finally reach a GVL yield of about 50% after 1 hour at 160 °C.

Each solution recovered at the end of reaction was analyzed by means of GC-MS, in order to identify possible organic by-products. All chromatograms show similar patterns, differing in the relative amounts of the components. As a representative example, the chromatogram of the reaction carried out at 120 °C for 30 minutes in the presence of [**1**]NO_3 is shown in the Supporting Information, together with the mass spectra of the detected species (Figures S25-S32). The identification of the mixture components has allowed us to suppose the reaction pathways reported in the Scheme 4.

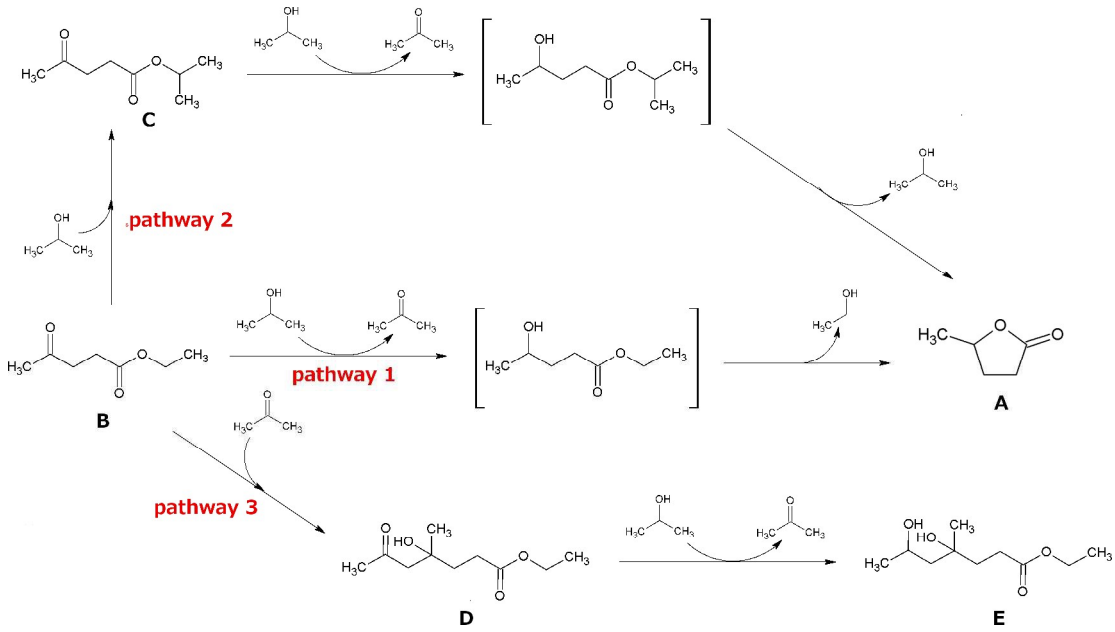

Scheme 4. General reaction pathways identified in the temperature range 120-160°C in the presence of [**1-4**]NO_3 as catalytic precursors.

According to Scheme 4, EL can engage several reactions in addition to the desired TH mechanism to GVL (pathway 1). In fact, it can undergo the trans-esterification reaction with the solvent, giving isopropyl levulinate (compound **C**), identified by GC-MS analysis (Figure S26), which can subsequently be converted to GVL through the TH mechanism, according to pathway 2, supposed also in the literature [7g,h,33]. Moreover, when TH takes place, acetone deriving from the oxidation of 2-

View Article Online
DOI: 10.1039/C8NJ03569E

propanol is present in the reaction medium and it can react with EL giving compounds **D** and **E**, both identified by GC-MS (Figures S29 and S30), according to pathway 3 [33].

On this basis, it is possible to rationalize the catalytic results. In fact, by the recorded chromatograms, it is possible to observe that the formation of compound **D** is higher in the presence of [**1**]NO_3 than with [**4**]NO_3 when the reaction was carried out at 120 °C (compare Figure S25 with Figure S31). Taking into account that compound **D** derives from the reaction between EL and acetone, this last one originating from the TH cycle, the higher amount of **D** ascertained with complex [**1**]NO_3 could underline that the TH mechanism is more active with system [**1**]NO_3 than [**4**]NO_3 at 120°C, leading to a higher GVL yield (Figure 4a). On the other hand, as already observed in Figure 4, the rise of the reaction temperature from 120 to 140°C seems to promote the TH mechanism also in the presence of complex [**4**]NO_3 and this is confirmed by the increase of the compound **D** in the run catalyzed by [**4**]NO_3 performed at 140°C respect to 120°C (compare Figures S31 and S32).

Once identified the most promising catalytic precursor ([**4**]NO_3) and the optimal reaction conditions (T = 160 °C, t = 60 minutes), the possible effect of the nature of the base was investigated. More precisely, the reaction was performed respectively in the presence of a metal hydroxide (NaOH or KOH), pyridine (Py) or triethylamine (NEt_3), which are four of the most investigated bases for the HT reaction in the presence of homogeneous catalysts [7d,34]. The results are reported in Table 4.

Table 4. Transfer hydrogenation conversion of EL (5 mmol) to GVL in 2-propanol (10 mL) using different bases (1 mol% respect to EL). Catalytic precursor [**4**]NO_3 (0.56 mol% respect to EL); MW heating; T = 160 °C; time = 60 min.

Run	Base	EL conversion (%)	GVL selectivity (%)	GVL yield (%)
7	NaOH	58.2	84.5	49.2
8	KOH	65.7	81.8	53.7
9	NEt_3	66.3	43.2	28.6
10	Pyridine	34.3	12.0	4.1

View Article Online
DOI: 10.1039/C8NJ03569E

KOH performed as the best base, providing values of conversion and yield slightly higher than those obtained with NaOH. Triethylamine determined a good conversion but a low selectivity. Instead, pyridine was not effective in terms of both conversion and selectivity. The trends observed for ethyl levulinate conversion (NEt_3 > KOH > NaOH > pyridine) and GVL yield (KOH > NaOH > NEt_3 > pyridine), respectively, are in alignment with previous findings on the same reaction catalyzed by iron complexes (see Introduction) [7d,35].

We finally tested [**4**]PF_6 and [**4**]BPh_4 as catalytic precursors, under the optimized reaction conditions (Table 5). The role of the counter anion revealed to be crucial, and the use of [**4**]PF_6 or [**4**]BPh_4 in the place of the homologous nitrate salt led to a significant increase in ethyl levulinate conversion. In addition, [**4**]BPh_4 maintained high GVL selectivity, providing the best GVL yield within the present work (about 62%), together with a productivity towards to GVL of 110 h^{-1} (measured as $mol_{GVL} \cdot mol_{Ru}^{-1} \cdot h^{-1}$). It is noteworthy that this productivity is higher than that achieved by Dai et al. starting from the same substrate to GVL in the presence of iron(II)-cyclopentadienone-tricarbonyl system under TH mechanism, which resulted equal to 5 h^{-1} (measured as $mol_{GVL} \cdot mol_{Fe}^{-1} \cdot h^{-1}$). Also in the case of [**4**]BPh_4, the important influence of the base was verified (Table 5, runs 12 and 13).

Table 5. Effect of the anion of the catalytic precursors in the conversion of EL (5 mmol) to GVL in 2-propanol (10 mL). Catalytic precursor (0.56 mol% respect to EL); KOH (1 mol% respect to EL); MW heating; T = 160 °C; t = 60 min. [a] Without base.

Run	Catalytic Precursor	EL conversion (%)	GVL selectivity (%)	GVL yield (%)
8	[**4**]NO_3	65.7	81.8	53.7
11	[**4**]PF_6	89.2	32.7	29.2
12	[**4**]BPh_4	81.4	75.8	61.7
13[a]	[**4**]BPh_4	75.2	41.2	31.0

View Article Online
DOI: 10.1039/C8NJ03569E

According to spectroscopic and GC-MS experiments (see SI for details), the complexes undergo ligand exchange/modification in the course of the hydrogenation reactions. On account of the important role played by the α-diimine moiety and the counterion, it is presumable that the active catalytic species are not dissimilar from the starting Ru compounds, and that progressive thermal degradation finally leads to inactive Ru species lacking of α-diimine and *p*-cymene ligands [36].

Conclusions

Cationic ruthenium arene compounds with α-diimine ligands have been synthesized, characterized and employed for the first time as catalytic precursors in the transfer hydrogenation (from isopropanol) for the conversion of ethyl levulinate into γ-valerolactone, i.e. a key reaction within the biorefinery route, assisted by microwave irradiation. A screening of α-diimines, counterions, base activators, reaction times and temperatures was carried out, leading to the definition of optimal reaction parameters. The results suggest that the anion and the α-diimine have a strong impact on the catalytic performances. Compound $[(\eta^6\text{-}p\text{-cymene})RuCl\{\kappa^2N\text{-}(4\text{-}C_6H_{10}OH)N{=}CHCH{=}N(4\text{-}C_6H_{10}OH)\}]BPh_4$ was found to act as the best catalytic precursor, which enables us to afford under sustainable conditions (only 1 mol% of base and 60 minutes reaction time), a γ-valerolactone yield of 62%, highlighting, for the first time, the promising potentialities of these complexes to be employed in an integrated bio-refinery approach.

Experimental

1) General experimental details.

All reagents and solvents were obtained from Alfa Aesar, Sigma Aldrich or TCI Europe and were used without further purifications. Ligands *N*,*N*′-bis(4-metylphenyl)ethylenediimine (**L1**),[19] *N*,*N*′-bis(4-hydroxyphenyl)ethylenediimine (**L2**),[20] *N*,*N*′-bis(cyclohexyl)ethylenediimine (**L3**),[20,19] *N*,*N*′-bis(4-hydroxycyclohexyl)ethylenediimine (**L4**)[20] and *N*,*N*′-bis(*tert*-butyl)ethylenediimine (**L5**)[19] were prepared as previously described; spectroscopic data for **L1** and **L5** are given in the Supporting

View Article Online
DOI: 10.1039/C8NJ03569E

Information. Needle-shaped X-ray quality crystals of **L2** were obtained from a DMSO solution layered with H_2O and settled aside at 4 °C. Compounds $[(\eta^6\text{-}p\text{-cymene})RuCl_2]_2$ [37] and $[(\eta^6\text{-}p\text{-cymene})RuCl\{\kappa^2N\text{-}(HCNR)_2\}]NO_3$ (R = 4-C_6H_4OH, [**2**]NO_3; C_6H_{11}, [**3**]NO_3; 4-$C_6H_{10}OH$, [**4**]NO_3) were prepared according to the published procedures [20]. All synthetic manipulations were performed in air with common laboratory glassware. Once isolated, [**5**]NO_3 was stored under N_2, all the other products being air-stable. NMR spectra were recorded on a Bruker Avance II DRX400 instrument equipped with a BBFO broadband probe at 25 °C, unless otherwise specified. Chemical shifts (expressed in parts per million) are referenced to the residual solvent peaks [38] (^1H, ^{13}C) or to external standards (^{19}F to $CFCl_3$, ^{31}P to 85% H_3PO_4, ^{35}Cl to 1 M NaCl in D_2O). In D_2O:CD_3OD solutions, chemical shifts were referenced to the residual HDO peak as in pure D_2O (δ_H = 4.79 ppm) [38]. Spectra were assigned with the assistance of DEPT-135 spectra and ^1H-^1H (COSY), ^1H-^{13}C (*gs*-HSQC and *gs*-HMBC) correlation experiments [39]. NMR signals in braces {} indicate superimpositions with other species. Infrared spectra were recorded on a Perkin Elmer Spectrum One FT-IR spectrometer, equipped with a UATR sampling accessory. UV-Vis spectra were recorded on an Ultraspec 2100 Pro spectrophotometer with 0.1 cm quartz cuvettes. IR and UV-Vis spectra were processed with Spectragryph software [40]. Carbon, hydrogen and nitrogen analysis was performed on a Vario MICRO cube instrument (Elementar). The chloride content in [**6**]PF_6 was determined with $AgNO_3$ potentiometric titration on a solution prepared by dissolution of the solid sample (*ca.* 20 mg) in acetone (1 mL) then diluted with H_2O (10 mL). The method was tested on $[(\eta^6\text{-}p\text{-cymene})RuCl_2]_2$ as a reference compound (Anal. calcd. for $C_{20}H_{28}Cl_4Ru_2$: Cl, 23.16. Found: 23.0; the compound was dissolved in a small volume of CH_2Cl_2, diluted with EtOH and then with H_2O). Melting points/decomposition temperatures were determined on a STMP3 Stuart scientific instrument with a capillary apparatus. pH measurements were performed with an Orion pH-meter equipped with a Hamilton glass pH-electrode, routinely calibrated with pH = 4.0 and pH = 7.0 buffer solutions (Sigma-Aldrich). Conductivity measurements were carried out at 21 °C using an XS COND 8 instrument (cell constant = 1.0 cm^{-1}) [41]. *Molar conductivity of reference 1:1*

View Article Online
DOI: 10.1039/C8NJ03569E

electrolytes. **$NaNO_3$**. Λ_m (MeOH, c = $1.7\cdot10^{-3}$ M): 119 $S\cdot cm^2\cdot mol^{-1}$. **NaCl**. Λ_m (MeOH, c = $3\cdot10^{-3}$ M) = 85 $S\cdot cm^2\cdot mol^{-1}$. **$KPF_6$**. Λ_m (MeOH, c = $2.7\cdot10^{-3}$ M): 108 $S\cdot cm^2\cdot mol^{-1}$. **$NaBPh_4$**. Λ_m (MeOH, c = $1.1\cdot10^{-3}$ M): 107 $S\cdot cm^2\cdot mol^{-1}$.

2) Synthesis and characterization of Ru compounds

[(η^6-*p*-cymene)RuCl{κ^2*N*-(HCN(4-C_6H_4Me))$_2$}]NO_3, [1]NO_3 (Chart 1).

Chart 1. Structure of [**1**]NO_3 (numbering refers to carbon atoms).

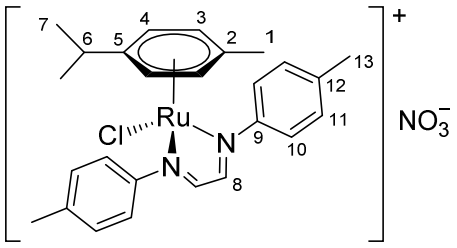

A brick red suspension of [(η^6-*p*-cymene)$RuCl_2$]$_2$ (204 mg, 0.333 mmol) and $AgNO_3$ (113 mg, 0.665 mmol) in MeCN (3 mL) was stirred at ambient temperature for 1 hour under protection from the light. During this time, the mixture turned orange with the precipitation of a colorless solid (AgCl). Therefore, the suspension was filtered over celite and **L1** (158 mg, 0.669 mmol) was added to the orange filtrate solution. The mixture was stirred at reflux temperature and the progress of reaction was checked by TLC ($KMnO_4$ stain). After 4 hours, the dark brown solution was cooled to ambient temperature and volatiles were removed under vacuum. The residue was suspended in Et_2O (20 mL) and the suspension was filtered. The resulting dark brown solid was washed with Et_2O and dried under vacuum (40 °C). Yield: 340 mg, 90%. On the other hand, a mixture of (*p*-cymene)Ru compounds containing *ca.* 70% [**1**]$^+$ (^{1}H NMR) was obtained when the reaction was performed in MeOH at ambient temperature. Compound [**1**]NO_3 is soluble in water and chlorinated solvents, poorly soluble in Et_2O and insoluble in hexane. Crystals suitable for X-ray analysis were obtained from CH_2Cl_2 solutions of [**1**]NO_3 layered with heptane or Et_2O and settled aside at -20 °C. Anal. calcd. for $C_{26}H_{30}ClN_3O_3Ru$: C, 54.88; H, 5.31; N, 7.38. Found: C, 54.69; H, 5.26; N, 7.48. T_m/°C > 200. IR (solid state): $\tilde{\upsilon}/cm^{-1}$ = 3059w, 2968w, 2925w,

View Article Online
DOI: 10.1039/C8NJ03569E

2872w, 1603w ($\nu_{C=N}$), 1567w, 1539w, 1502m, 1471m, 1381m-sh, 1345s, 1330s-br (ν_{NO3}), 1310s, 1216m, 1176w, 1162w, 1112w, 1093w, 1054w, 1038w, 1023m, 959w, 907w, 881m, 842w-sh, 818s, 773m, 732w, 711w, 676w. UV-Vis (CH_2Cl_2, c = $1.0\cdot10^{-3}$ M): λ_{max}/nm ($\varepsilon/M^{-1}\cdot cm^{-1}$) = 371 ($1.2\cdot10^4$), 450sh ($4.0\cdot10^3$), 550sh ($1.1\cdot10^3$). Λ_m (c = $1.0\text{-}1.1\cdot10^{-3}$ M) = 15 (CH_2Cl_2); 119 (MeOH) $S\cdot cm^2\cdot mol^{-1}$. ^{1}H NMR ($CDCl_3$): δ/ppm = 8.43 (s, 2H, C8-H), 7.81 (d, $^3J_{HH}$ = 7.9 Hz, 4H, C10-H), 7.32 (d, $^3J_{HH}$ = 7.6 Hz, 4H, C11-H), 5.18 (pseudo-q, $^3J_{HH}$ = 6.2 Hz, 4H, C3-H + C4-H), 2.74 (hept, $^3J_{HH}$ = 6.7 Hz, 1H, C6-H), 2.46 (s, 6H, C13-H), 2.20 (s, 3H, C1-H), 1.19 (d, $^3J_{HH}$ = 6.8 Hz, 6H, C7-H). No change in the ^{1}H spectrum was observed after 5 days at ambient temperature. ^{13}C NMR ($CDCl_3$): δ/ppm = 165.9 (C8), 150.4 (C9), 141.1 (C12), 130.2 (C11), 122.8 (C10), 110.5 (C5), 102.8 (C2), 88.3 (C3), 86.6 (C4), 31.0 (C6), 22.4 (C7), 21.5 (C13), 18.9 (C1).

[(η^6-*p*-cymene)RuCl{κ^2*N*-(HCN^{t}Bu)$_2$}]NO$_3$, [5]NO$_3$ (Chart 2).

Chart 2. Structure of [**5**]NO_3 (numbering refers to carbon atoms).

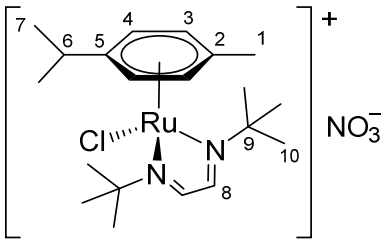

The synthesis was carried out as described for [**1**]NO_3, using [(η^6-*p*-cymene)$RuCl_2]_2$ (50 mg, 0.082 mmol), $AgNO_3$ (28 mg, 0.16 mmol) and **L5** (29 mg, 0.17 mmol) in MeCN (3 mL). After 3 hours, the orange solution was cooled to ambient temperature and volatiles were removed under vacuum. The residue was suspended in Et_2O (20 mL) and the suspension was filtered. The resulting orange-brown solid was washed with Et_2O, dried under vacuum (40 °C) and stored under nitrogen (hygroscopic). Yield: 75 mg, 92%. On the other hand, a mixture of compounds containing unreacted **L5** was obtained when the reaction was performed in MeOH at room or reflux temperature. Compound [**5**]NO_3 is soluble in water and chlorinated solvents, insoluble in Et_2O, hexane. Anal. calcd. for $C_{20}H_{34}ClN_3O_3Ru$: C,

View Article Online
DOI: 10.1039/C8NJ03569E

47.94; H, 6.84; N, 8.39. Found: C, 48.02; H, 6.76; N, 8.47. IR (solid state): $\tilde{\upsilon}/cm^{-1}$ = 3600-3200w-br, 2973m, 2936m, 2876w, 1870w, 1626m ($\nu_{C=N}$), 1539w, 1478m, 1463m, 1369s, 1323s-br (ν_{NO3}), 1224m, 1177s, 1090m, 1057m, 1038m, 977m, 927w, 879m, 829m, 806w, 732w, 694w, 671w. UV-Vis (CH_2Cl_2, c = $1.9\cdot10^{-3}$ M): λ_{max}/nm ($\varepsilon/M^{-1}\cdot cm^{-1}$) = 278 ($2.7\cdot10^3$), 378 ($1.7\cdot10^3$), 431 ($1.5\cdot10^3$). Λ_m (CH_2Cl_2, c = $1.9\cdot10^{-3}$ M) = 8.9 $S\cdot cm^2\cdot mol^{-1}$. ^{1}H NMR ($CDCl_3$, 55 °C): δ/ppm = 8.72 (s-br, 2H, C8-H), 5.95–5.82 (m-br, 4H, C3-H + C4-H), 2.88 (m-br, 1H, C6-H), 2.30 (s, 3H, C1-H), 1.68 (s, 18H, C10-H), 1.26 (m-br, 6H, C7-H). The ^{1}H spectrum recorded at 25 °C displays broader resonances. $^{13}C\{^1H\}$ NMR ($CDCl_3$, 353 K): δ/ppm = 168.5 (C8), 68.6 (C9), 82* (br, C3 + C4), 32.2 (C10), 31.9 (C6), 22.5* (br, C7), 18.7* (br, C1). ^{13}C signals for the *p*-cymene ligand (*) were too broad to be directly observed; they were identified through *gs*-HSQC experiment.

[(η^6-*p*-cymene)RuCl(MeCN)$_{0.66}$]PF_6, [6]PF_6.

The mixture of chlorido-acetonitrile complexes obtained by the following procedure is treated as a single compound with formula [(η^6-*p*-cymene)RuCl(MeCN)$_{0.66}$]PF_6 for the sake of simplicity.

A brick red suspension of [(η^6-*p*-cymene)$RuCl_2$]$_2$ (300 mg, 0.490 mmol) and NH_4PF_6 (160 mg, 0.982 mmol) in MeCN (4 mL) was stirred at ambient temperature for 14 hours. During this time, the mixture turned orange with the precipitation of a colorless solid (NH_4Cl). The suspension was filtered over celite then volatiles were removed from the orange filtrate solution, affording an oily orange residue. At this point, literature procedures[26a,b] prescribe a slow crystallization with Et_2O to obtain [(η^6-*p*-cymene)RuCl(MeCN)$_2$]PF_6 as an orange powder. Instead, the oil was re-dissolved in few mL of CH_2Cl_2 and a foamy orange solid was readily obtained upon solvent removal under vacuum (40 °C). Yield: 430 mg, 99%. The compound is soluble in MeCN, CH_2Cl_2, poorly soluble in $CHCl_3$, MeOH and insoluble in Et_2O, hexane. Anal. calcd. for $C_{10}H_{14}ClF_6PRu(CH_3CN)_{0.66}$: C, 30.70; H, 3.64; N, 2.09; Cl, 8.00. Found: C, 30.76; H, 3.55; N, 2.16; Cl, 8.0. IR (solid state): $\tilde{\upsilon}/cm^{-1}$ = 3090w, 2973w, 2944w, 2876w, 2374-2345w ($\nu_{C\equiv N}$), 2329w ($\nu_{C\equiv N}$), 2301w ($\nu_{C\equiv N}$), 1538w, 1504w, 1473m, 1446w, 1393m, 1328w, 1282w,

View Article Online
DOI: 10.1039/C8NJ03569E

1202w, 1117w, 1092w, 1059w, 1033w, 1008w, 877m-sh, 826vs (ν_{PF6}), 740m-sh, 673w. ^{1}H NMR (CD_3CN): three Ru compounds (**6a**, **6b**, **6c**) in 70:15:15 molar ratio; overall MeCN/*p*-cymene ratio = 0.66. ***6a***. δ/ppm = 5.83, 5.58 (d, $^3J_{HH}$ = 6.1 Hz, 4H, Ru-CH); 2.88 (hept, $^3J_{HH}$ = 6.8 Hz, 1H, C<u>H</u>Me$_2$), 2.49 (s, 2H, Ru-NCMe), 2.23 (s, 3H, Ru-CMe), 1.30 (d, $^3J_{HH}$ = 6.9 Hz, 6H, CH<u>Me</u>$_2$). ***6b, 6c***. δ/ppm = 6.10, 5.87, 5.55, 5.30 (d, $^3J_{HH}$ = 6.0 Hz; 4H, Ru-CH); {2.88 (C<u>H</u>Me$_2$)}, 2.27, 2.18 (s, 3H, Ru-CMe); 2.14 (s, 4H, Ru-NCMe), {1.30 (CH<u>Me</u>$_2$)}. ^{1}H NMR (CD_2Cl_2): two Ru compounds (**6a'**, **6b'**) with 77:23 molar ratio + uncoordinated MeCN (δ/ppm = 1.84(br.)). ***6a'***. δ/ppm = 5.64, 5.46 (d, $^3J_{HH}$ = 6.0 Hz, 4H, Ru-CH); 2.78 (hept, $^3J_{HH}$ = 6.9 Hz, 1H, C<u>H</u>Me$_2$), 2.55 (s, 3H, Ru-NCMe), 2.22 (s, 3H, Ru-CMe), 1.30 (d, $^3J_{HH}$ = 6.9 Hz, 6H, CH<u>Me</u>$_2$). ***6b'***. δ/ppm = 6.12, 5.92 (d, $^3J_{HH}$ = 6.2 Hz, 4H, Ru-CH); 2.86 (hept, $^3J_{HH}$ = 6.8 Hz, 1H, C<u>H</u>Me$_2$), 2.33 (s, 3H, Ru-CMe), 2.12, 1.97 (s, 3H, Ru-NCMe); 1.36-1.33 (m, 6H, CH<u>Me</u>$_2$). ^{13}C{^{1}H} NMR (CD_2Cl_2, ***6a'***): δ/ppm = 102.3 (C<u>^{i}</u>Pr), 97.6 (Ru-<u>C</u>Me), 79.3, 78.5 (Ru-CH); 31.8 (<u>CH</u>Me$_2$), 22.2 (CH<u>Me</u>$_2$), 19.1 (Ru-C<u>Me</u>), 4.1 (Ru-NC<u>Me</u>). ^{31}P{^{1}H} NMR (CD_2Cl_2): δ/ppm −144.5 (hept, $^1J_{PF}$ = 711 Hz, PF_6^-).

[(η^6-*p*-cymene)RuCl{κ^2*N*-(HCN(4-C$_6$H$_4$OH))$_2$}]PF$_6$, [2]PF$_6$ (Chart 3).

Chart 3. Structure of [**2**]PF_6, (numbering refers to carbon atoms).

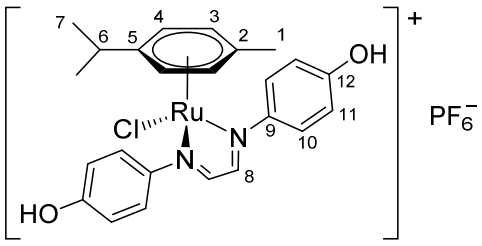

[(η^6-*p*-cymene)RuCl(MeCN)$_{0.66}$]PF_6 (325 mg, 0.734 mmol) and **L2** (176 mg, 0.733 mmol) were dissolved in MeOH (5 mL) with immediate darkening of the mixture. The solution was stirred at ambient temperature for 3 hours then volatiles were removed under vacuum. The residue was suspended in Et_2O and the suspension was filtered. The black solid was washed with Et_2O and dried under vacuum (40 °C) over P_2O_5. Yield: 390 mg, 81%. Compound [**2**]PF_6 is highly soluble in acetone, soluble in

View Article Online
DOI: 10.1039/C8NJ03569E

water, DMSO, methanol; insoluble in chlorinated solvents, Et_2O and hexane. Anal. calcd. for $C_{24}H_{26}ClF_6N_2O_2PRu$: C, 43.94; H, 4.00; N, 4.27. Found: C, 44.03; H, 3.89; N, 4.40. IR (solid state): $\tilde{\upsilon}/cm^{-1}$ = 3544w ($\nu_{O\text{-}H}$), 3400-3100w-br ($\nu_{O\text{-}H}$), 3073w, 2967w, 2933w, 2878w, 2810w, 1709w, 1605m ($\nu_{C=N}$), 1591m, 1571m, 1562m-sh, 1505s, 1472m, 1447m, 1368w, 1271s, 1210s, 1165s, 1137w, 1105w, 1056w, 1024m, 996w, 959w, 831vs-br (ν_{PF6}), 740m, 721w, 673w. UV-Vis (MeOH, c = $1.1\cdot10^{-3}$ M): λ_{max}/nm ($\varepsilon/M^{-1}\cdot cm^{-1}$) = 268 ($1.1\cdot10^4$), 422 ($1.3\cdot10^4$), 550-575br ($2.9\cdot10^3$). Λ_m (MeOH, c = $1.1\cdot10^{-3}$ M) = 71 $S\cdot cm^2\cdot mol^{-1}$. ^{1}H NMR (DMSO-$d_6$): δ/ppm = 10.4 (s, 2H, OH), 8.47 (s, 2H, C8-H), 7.66 (d, $^3J_{HH}$ = 8.7 Hz, 4H, C10-H), 6.98 (d, $^3J_{HH}$ = 8.7 Hz, 4H, C11-H), 5.49 (pseudo-q, $^3J_{HH}$ = 6.4 Hz, 4H, C3-H + C4-H), 2.30 (hept, $^3J_{HH}$ = 6.9 Hz, 1H, C6-H), 2.23 (s, 3H, C1-H), 0.96 (d, $^3J_{HH}$ = 6.9 Hz, 6H, C7-H). No change in the ^{1}H spectrum was observed after 43 days at ambient temperature. $^{13}C\{^1H\}$ NMR (DMSO-d_6): δ/ppm = 162.4 (C8), 159.8 (C12), 143.9 (C9), 124.3 (C10), 115.8 (C11), 106.6 (C5), 105.8 (C2), 88.7 (C4), 86.9 (C3), 30.7 (C6), 21.5 (C7), 18.5 (C1). $^{19}F\{^1H\}$ NMR (DMSO-d_6): δ/ppm = −70.2 (d, $^1J_{FP}$ = 711 Hz, PF_6^-). $^{31}P\{^1H\}$ NMR (DMSO-d_6): δ/ppm = −144.2 (hept, $^1J_{PF}$ = 711 Hz, PF_6^-).

[(η^6-*p*-cymene)RuCl{κ^2*N*-(HCN(4-$C_6H_{10}OH$))$_2$}]X, [4]X (X = PF_6, BPh_4) (Chart 4).

Chart 4. Structure of [**4**]X (X = PF_6, BPh_4) (numbering refers to carbon atoms).

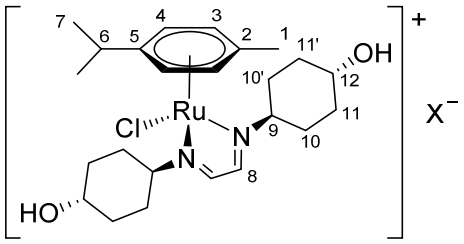

[4]PF_6. A suspension of [(η^6-*p*-cymene)RuCl$(MeCN)_{0.66}$]PF_6 (100 mg, 0.226 mmol) and **L4** (57 mg, 0.23 mmol) in MeCN (5 mL) was stirred at reflux temperature for 9 hours and the progress of reaction was monitored via ^{1}H NMR. Therefore the red mixture was allowed to cool to ambient temperature and was filtered over celite. Volatiles were removed under vacuum from the filtrate solution and the residue was suspended in Et_2O. The suspension was filtered and the resulting orange-red solid was washed with

View Article Online
DOI: 10.1039/C8NJ03569E

Et_2O and dried under vacuum (40 °C) over P_2O_5. Yield: 137 mg, 91%. On the other hand, a mixture of (*p*-cymene)Ru compounds containing minor amounts of $[\mathbf{4}]^+$ (^{1}H NMR) was obtained when the reaction was performed *one-pot* with $[(\eta^6\text{-}p\text{-cymene})RuCl_2]_2$, **L4** and NH_4PF_6 (1:1:1 mol ratio) in MeCN at ambient temperature. Compound [**4**]PF_6 is soluble in acetone, H_2O, DMSO and MeOH; insoluble in chlorinated solvents, Et_2O and hexane. Anal. calcd. for $C_{24}H_{38}ClF_6N_2O_2PRu$: C, 43.14; H, 5.73; N, 4.19. Found: C, 42.90; H, 5.82; N, 4.30. IR (solid state): $\tilde{\upsilon}/cm^{-1}$ = 3587w ($\nu_{O\text{-}H}$), 3410w-br ($\nu_{O\text{-}H}$), 3086w-br, 2964w, 2938w, 2904m, 2866w, 1640w-br ($\nu_{C=N}$), 1538w, 1508w, 1471w-sh, 1455m, 1406w, 1392w, 1368w, 1326w, 1284w, 1230w, 1203w, 1081m, 1056m, 964w, 905w, 877m-sh, 833vs (ν_{PF6}), 740w. UV-Vis (MeOH, c = $1.6\cdot10^{-3}$ M): λ_{max}/nm ($\varepsilon/M^{-1}\cdot cm^{-1}$) = 277 ($3.4\cdot10^3$), 372sh ($2.0\cdot10^3$), 426 ($2.9\cdot10^3$). Λ_m (MeOH, c = $1.6\cdot10^{-3}$ M) = 116 $S\cdot cm^2\cdot mol^{-1}$. ^{1}H NMR ($CD_3OD$): δ/ppm = 8.33 (s, 2H, C8-H), 6.18 (d, $^3J_{HH}$ = 6.0 Hz, 2H, C4-H), 5.81 (d, $^3J_{HH}$ = 5.9 Hz, 2H, C3-H), 4.49 (t, $^3J_{HH}$ = 11.2 Hz, 2H, C9-H), 3.64 (t, $^3J_{HH}$ = 10.5 Hz, 2H, C12-H), 2.77 (hept, $^3J_{HH}$ = 6.7 Hz, 1H, C6-H), 2.52 (d, *J* = 12.9 Hz, 2H, C10-H), 2.32–2.27 (m, 2H, C10'-H), 2.27 (s, 3H, C1-H), 2.13 (d, *J* = 12.0 Hz, 2H, C11'-H), 2.04 (d, *J* = 13.4 Hz, 2H, C11-H), 1.91 (q, *J* = 11.4 Hz, 2H, C10'-H'), 1.62 (q, *J* = 10.1 Hz, 2H, C11'-H'), 1.54 (q, *J* = 10.1 Hz, 2H, C11-H'), 1.37 (q, *J* = 11.2 Hz, 2H, C10-H'), 1.16 (d, $^3J_{HH}$ = 6.7 Hz, 6H, C7-H). $^{13}C\{^1H\}$ NMR (CD_3OD): δ/ppm = 165.3 (C8), 109.2 (C5), 108.4 (C2), 89.5 (C4), 87.3 (C3), 75.7 (C9), 70.1 (C12), 34.9 (C11), 34.5 (C11'), 34.0 (C10), 33.1 (C6), 32.1 (C10'), 22.7 (C7), 19.4 (C1). $^{19}F\{^1H\}$ NMR (CD_3OD): δ/ppm = −74.4 (d, $^1J_{FP}$ = 708 Hz, PF_6^-). $^{31}P\{^1H\}$ NMR (CD_3OD): δ/ppm = −146.7 (hept, $^1J_{PF}$ = 708 Hz, PF_6^-).

[4]BPh$_4$. A solution of [**4**]NO_3 (68 mg, 0.12 mmol) and Na[BPh_4] (40 mg, 0.12 mmol) in acetone (6 mL) was stirred for 14 hour at ambient temperature, affording a red-orange solution and a colorless precipitate ($NaNO_3$). The suspension was filtered over celite and volatiles were removed under vacuum from the filtrate solution. The residue was dissolved in CH_2Cl_2 (5 mL) and extracted with H_2O (10 mL). The red organic phase was separated and taken to dryness under vacuum. The resulting orange solid was suspended in Et_2O then filtered, washed with Et_2O and dried under vacuum (40 °C). Yield: 87 mg, 87%.

View Article Online
DOI: 10.1039/C8NJ03569E

Compound [**4**]BPh_4 is soluble in CH_2Cl_2, MeOH and MeCN, poorly soluble in $CHCl_3$ and insoluble in Et_2O, H_2O. Anal. calcd. for $C_{48}H_{58}BClN_2O_2Ru$: C, 68.44; H, 6.94; N, 3.32. Found: C, 68.20; H, 7.05; N, 3.42. IR (solid state): $\tilde{\upsilon}/cm^{-1}$ = 3540w ($\nu_{O\text{-}H}$), 3410w-br ($\nu_{O\text{-}H}$), 3055w, 3036w, 3000w, 2983w, 2964w, 2934m, 2861w, 2902w, 1579w, 1538w ($\nu_{C=N}$), 1478m, 1453m, 1426m, 1402w, 1388w, 1366m, 1328w, 1305w, 1267m, 1229w, 1201w, 1184w, 1138w, 1080s, 1054s, 1032m, 998w, 962m, 902w, 862m, 846m, 746m-sh, 733s (ν_{BPh4}), 704s (ν_{BPh4}). UV-Vis (MeOH, c = $1.4\cdot10^{-3}$ M): λ_{max}/nm ($\varepsilon/M^{-1}\cdot cm^{-1}$) = 265 ($7.5\cdot10^3$), 273 ($6.3\cdot10^3$), 277sh ($3.9\cdot10^3$), 369sh ($2.6\cdot10^3$), 427 ($3.4\cdot10^3$). Λ_m (MeOH, c = $1.4\cdot10^{-3}$ M) = 81 (MeOH) $S\cdot cm^2\cdot mol^{-1}$. ^{1}H NMR ($CD_2Cl_2$): δ/ppm = 7.41–7.34 (m-br, 8H, BPh_{meta}), 7.00 (t, $^3J_{HH}$ = 7.3 Hz, 8H, BPh_{ortho}), 6.83 (t, $^3J_{HH}$ = 7.1 Hz, 4H, BPh_{para}), 6.57 (s, 2H, C8-H), 5.52 (d, $^3J_{HH}$ = 6.2 Hz, 2H, C4-H), 5.30 (d, $^3J_{HH}$ = 6.5 Hz, 2H, C3-H), 3.97 (t, $^3J_{HH}$ = 11.4 Hz, 2H, C9-H), 3.64 (m-br, 2H, C12-H), 2.61 (hept, $^3J_{HH}$ = 6.7 Hz, 1H, C6-H), 2.37–2.28 (m, 2H, C10-H), 2.18 (s, 3H, C1-H), 2.17–2.11 (m, 2H, C11-H), 2.11–2.05 (m, 2H, C11'-H), 1.98–1.90 (m, 2H, C10'-H), 1.75 (s, 2H, OH), 1.52–1.32 (m, 6H, C10'-H' + C11-H' + C11'-H'), 1.28–1.13 (m, 2H, C10-H'), 1.11 (d, $^3J_{HH}$ = 6.9 Hz, 6H, C7-H). $^{13}C\{^1H\}$ NMR (CD_2Cl_2): δ/ppm = 164.5 (q, $^1J_{CB}$ = 49.0 Hz, BPh_{ipso}), 164.1 (C8), 136.2 (BPh_{ortho}), 126.4 (BPh_{meta}), 122.6 (BPh_{para}), 108.1 (C5), 106.8 (C2), 87.7 (C4), 86.1 (C3), 75.2 (C9), 69.3 (C12), 34.7 (C11'), 34.3 (C11), 32.8 (C10), 32.1 (C6), 31.2 (C10'), 22.6 (C7), 19.5 (C1). ^{1}H NMR (CD_3OD): δ/ppm = 7.63 (s, 2H, C8-H), 7.33–7.27 (m, 8H, BPh_{meta}), 6.95 (t, $^3J_{HH}$ = 7.4 Hz, 8H, BPh_{ortho}), 6.82 (t, $^3J_{HH}$ = 7.2 Hz, 4H, BPh_{para}), 6.02 (d, $^3J_{HH}$ = 6.4 Hz, 2H, C4-H), 5.65 (d, $^3J_{HH}$ = 6.3 Hz, 2H, C3-H), 4.33 (t, $^3J_{HH}$ = 11.5 Hz, 2H, C9-H), 3.66–3.57 (m, 2H, C12-H), 2.69 (hept, $^3J_{HH}$ = 6.9 Hz, 1H, C6-H), 2.46–2.40 (m, 2H, C10-H), 2.18 (s, 3H, C1-H), 2.15–2.07 (m, 4H, C11-H + C11'-H), 2.06–1.99 (m, 2H, C10'-H), 1.76–1.64 + 1.63–1.43 (m, 6H; C10'-H' + C11-H' + C11'-H'), 1.32–1.23 (m, 2H, C10-H'), 1.12 (d, $^3J_{HH}$ = 6.9 Hz, 6H, C7-H). No change was observed in the ^{1}H spectrum after 3 days at ambient temperature. $^{13}C\{^1H\}$ NMR (CD_3OD): δ/ppm = 165.3 (C8), 137.3 (BPh_{ortho}), 126.6 (BPh_{meta}), 122.9 (BPh_{para}), 108.9 (C5), 108.4 (C2), 89.4 (C4), 87.1 (C3), 75.6 (C9), 70.0 (C12), 34.9 (C11'), 34.5 (C11), 33.8 (C10), 33.0 (C6), 32.0 (C10'), 22.7 (C7), 19.4 (C1).

View Article Online
DOI: 10.1039/C8NJ03569E

3) X-ray crystallography.

Crystal data and collection details for **L2** and [**1**]NO_3 are reported in Table 6. Data were recorded on a Bruker APEX II diffractometer equipped with a PHOTON100 detector using Mo–Kα radiation. Data were corrected for Lorentz polarization and absorption effects (empirical absorption correction SADABS) [42]. The structures were solved by direct methods and refined by full-matrix least-squares based on all data using F^2 [43]. Hydrogen atoms were fixed at calculated positions and refined by a riding model, except those bonded to O-atoms which have been located in the difference Fourier Map and refined isotropically. All non-hydrogen atoms were refined with anisotropic displacement parameters.

Table 6. Crystal data and measurement details for **L2** and **[1]**NO_3.

Compound	**L2**	**[1]NO_3**
Formula	$C_{14}H_{12}N_2O_2$	$C_{26}H_{30}ClN_3O_3Ru$
FW	240.26	569.05
T, K	100(2)	100(2)
λ, Å	0.71073	0.71073
Crystal system	Monoclinic	Monoclinic
Space group	$P2_1/c$	$P2_1/c$
a, Å	4.9045(11)	9.8785(6)
b, Å	11.022(2)	13.9080(9)
c, Å	10.913(3)	18.1728(11)
β, °	101.589(6)	101.9450(10)
Cell Volume, Å^3	577.9(2)	2442.7(3)
Z	2	4
D_c, g·cm^{-3}	1.381	1.547
μ, mm^{-1}	0.094	0.785
F(000)	252	1168
Crystal size, mm	0.19 x 0.16 x 0.14	0.18 x 0.16 x 0.12
θ limits, °	2.654 – 26.999	1.859 – 25.049
Reflections collected	6473	28024
Independent reflections	1260 (R_{int} = 0.0401)	4323 (R_{int} = 0.0471)

View Article Online
DOI: 10.1039/C8NJ03569E

Data / restraints /parameters	1260 / 0 / 83	4323 / 108 / 344
Goodness of fit on F^2	1.045	1.107
R_1 ($I > 2\sigma(I)$)	0.0439	0.0437
wR_2 (all data)	0.1025	0.0984
Largest diff. peak and hole, e Å^{-3}	0.247 and –0.296	2.808 and –0.825

4) Catalytic study.

Catalytic conversion of ethyl levulinate (EL) to γ-valerolactone (GVL).

The catalytic reaction was performed in a monomodal microwave reactor CEM Discover S-class System. In a typical run, ethyl levulinate (5 mmol), 2-propanol (10 mL) acting as hydrogen donor and solvent, the base (0.05 mmol) and the proper amount of catalyst were charged in a 35 mL reactor vessel. The mixture was heated at the stated temperature during the established time under magnetic stirring. Then, the reactor was rapidly cooled to ambient temperature through an external air flow, and the samples were collected and analyzed by gas chromatography.

Sample analysis.

EL conversion (%) and GVL yield (%), expressed respectively as $[(mol^{in}_{EL} - mol^{fin}_{EL})/mol^{in}_{EL}]*100$ and $(mol_{GVL}/mol^{in}_{EL})*100$, were quantified by gas chromatography with DANI GC1000 instrument equipped with FID detector and HP-PONA capillary column (50 m × 0.2 mm × 0.5 μm) 100% dimethylpolysiloxane. Nitrogen was employed as carrier gas, with flow = 1 mL min^{-1}. The injector and detector temperatures were both maintained at 250 °C, and the following temperature program was adopted for the chromatographic run: 60 °C isothermal for 2 min; 10 °C/min up to 230 °C; 230 °C isothermal for 5 min. 1-hexanol was employed as internal standard for analysis. The products present in the reaction solution were identified by GC-MS (Agilent 7890B-5977A) with HP-5MS capillary column (30 m × 0.25 mm × 0.25 μm) (5%-phenyl)-methylpolysiloxane. Helium was employed as carrier gas, with flow = 1 mL min^{-1}. The injector and detector temperatures were maintained at 250 °C and 280 °C,

View Article Online
DOI: 10.1039/C8NJ03569E

respectively, and the following temperature program was adopted for the chromatographic run: 40 °C isothermal for 2 min; 10 °C/min up to 230 °C; 230 °C isothermal for 5 min.

Notes

The authors declare no competing financial interest.

Acknowledgement

We thank the *University of Pisa* (Fondi di Ateneo 2017) for financial support.

Supporting Information Available

Spectroscopic data, IR and NMR spectra of compounds, chromatograms and mass spectra, analysis of residues. CCDC reference numbers 1830401 (**L2**) and 1830402 ([**1**]NO_3) contain the supplementary crystallographic data for the X-ray studies reported in this paper. These data can be obtained free of charge at www.ccdc.cam.ac.uk/conts/retrieving.html (or from the Cambridge Crystallographic Data Centre, 12, Union Road, Cambridge CB2 1EZ, UK; fax: (internat.) +44-1223/336-033; e-mail: deposit@ccdc.cam.ac.uk).

View Article Online
DOI: 10.1039/C8NJ03569E

References

1 (a) N. Armaroli, V. Balzani, Chem. Asian J. 2011, 6, 768-784. (b) X. Tong, Y. Ma, Y. Li, Appl. Catal. A: Gen. 2010, 385, 1-13.

2 Recent reviews on the topic: (a) I. Bodachivskyi, U. Kuzhiumparambil, D. B. G. Williams, ChemSusChem 2018, 11, 642–660. (b) L. Yan, Q. Yao, Y. Fu, Green Chem. 2017, 19, 5527-5547. (c) U. Omoruyi, S. Page, J. Hallett, P. W. Miller, ChemSusChem 2016, 9, 2037-2047. (d) Z. Zhang, ChemSusChem 2016, 9, 156-171. (e) K. Yan, C. Jarvis, J. Gu, Y. Yan, Renew. Sustain. Energy Rev. 2015, 51, 986-997. (f) F. Liguori, C. Moreno-Marrodan, P. Barbaro, ACS Catal. 2015, 5, 1882−1894. (g) A.M. Raspolli Galletti, C. Antonetti, E. Ribechini, M. P. Colombini, N. Nassi o Di Nasso, E. Bonari, Appl. Energy 2013, 102, 157-162. (h) A. M. Raspolli Galletti, C. Antonetti, V. De Luise, M. Martinelli, Green Chem. 2012, 14, 688-694. (i) J. Molletti, M. S. Tiwari, G.D. Yadav, Chem. Eng. J. 2018, 334, 2488-2499. (j) Y. Zhang, Y. Ge, X. Wang, J. Chen, X. Huang, Y. Liao, ACS Omega 2017, 2, 3228-3240. (k) C. Antonetti, D. Licursi, S. Fulignati, G. Valentini, A.M. Raspolli Galletti, Catalysts 2016, 6, 196-224. (l) A.S. Piskun, J. Ftouni, Z. Tang, B.M. Weckhuysen, P.C.A. Bruijnincx, H. J. Heeres, Appl. Catal. A: Gen. 2018, 549, 197-206.

3 Selected references: (a) Y. Gu, F. Jérome, Chem. Soc. Rev. 2013, 42, 9550-9570. (b) I. T. Horvath, H. Mehdi, V. Fabos, L. Boda, L. T. Mika, Green Chem. 2008, 10, 238-242. (c) X. Tang, X. Zeng, Z. Li, L. Hu, Y. Sun, S. Lu, T. Lei, L. Lin, Renew. Sust. Ener. Rev. 2014, 40, 608-620. (d) A. Bohre, S. Dutta, B. Saha, M. M. Abu-Omar, ACS Sustain. Chem. Engin. 2015, 3, 1263-1277. (e) J.Q. Bond, A.A. Upadhye, H. Olcay, G.A. Tompsett, J. Jae, R. Xing, D.M. Alonso, D. Wang, T. Zhang, R. Kumar, A. Foster, S.M. Sen, C.T. Maravelias, R. Malina, S.R.H. Barrett, R. Lobo, C.E. Wyman, J.A. Dumesic, G.W. Huber, Energy Environ. Sci. 2014, 7, 1500-1523. (f) S. Liu, G. Fan, L. Yang, F. Li, Appl. Catal. A: Gen. 2017, 543, 180-188. (g) Z. Li, Y. Jiang, X. Tang, M. Zuo, X. Zeng, Y. Sun, L. Lin, RSC Adv. 2015, 5, 8297-8300. (h) Y.C. Ahn, J. Han, Biores. Technol. 2017, 245, 442-448.

4 See for instance: (a) S. Zhao, G. Xu, J. Chang, C. Chang, J. Bai, S. Fang, Z. Liu, Bioresources 2015, 10, 2223-2234. (b) X. Hu, S. Jiang, L. Wu, S. Wang, C. Z. Li, Chem. Commun. 2017, 53, 2938-2941. (c) P. Neves, M. M. Antunes, P. A. Russo, J. P. Abrantes, S. Lima, A. Fernaneds, M. Pillinger, S. M. Rocha, M. F. Ribeiro, A. A. Valente, Green Chem. 2013, 15, 3367-3376. (d) C. Chang, G. Xu, X. Jiang, Biores. Technol. 2012, 121, 93-99.

5 (a) C.A.M.R. Van Slagmaat, S.M.A. De Wildeman, Eur. J. Inorg. Chem. 2018, 694–702. (b) F. M. A. Gelilen, B. Engendahl, A. Harwardt, W. Marquardt, J. Klankermayer, W. Leitner, Angew. Chem. 2010, 122, 5642-5646. (c) P. C. A. Bruijnincx, B. M. Weckhuysen, Nat. Commun. 2015, 6, 6540-6549. (d) A. M. Ruppert, J. Grams, M. Jedrzejczyk, J. Matras-Michalska, N. Keller, K. Ostojska, P. Sautet, ChemSusChem 2015, 8, 1538-1547. (e) S. C. Patankar, G. D. Yadav, ACS Sustain. Chem. Engin. 2015, 3, 2619-2630.

View Article Online
DOI: 10.1039/C8NJ03569E

6 (a) A. M. Ruppert, M. Jędrzejczyk, O. Sneka-Płatek, N. Keller, A.S. Dumon, C. Michel, P. Sautet, J. Grams, Green Chem. 2016, 18, 2014-2028. (b) M.C. Fu, R. Shang, Z. Huang, Y. Fu, Synlett. 2014, 25, 2748-2752. (c) P.A. Son, S. Nishimura, K. Ebitani, RSC Adv. 2014, 4, 10525-10530.

7 (a) M. G. Al-Shaal, M. Calin, I. Delidovich, R. Palkovits, Catal. Commun. 2016, 75, 65-68. (b) A.S. Amarasekara, M.A. Hasan, Catal. Commun. 2015, 60, 5-7. (c) S. Xu, D. Yu, T. Ye, P. Tian, RSC Adv. 2017, 7, 1026-1031. (d) N. Dai, R. Shang, M. Fu, Y. Fu, Chin. J. Chem. 2015, 33, 405-408. (e) R. Wang, J. Wang, H. Zi, Y. Xia, H. Wang, X. Liu, Mol. Catal. 2017, 441, 168-178. (f) J. He, H. Li, Y.M. Lu, Y.X. Liu, Z.B. Wu, D.Y. Hu, S. Yang, Appl. Catal. A: Gen. 2016, 510, 11-19. (g) Y. Kuwahara, H. Kango, H. Yamashita, ACS Sustain. Chem. Eng. 2017, 5, 1141-1152. (h) F. Li, J. France, Z. Cai, Y. Li, S. Liu, H. Lou, J. Long, X. Li, Appl. Catal. B: Env. 2017, 214, 67-77. (i) Y. Kuwahara, W. Kaburagi, T. Fujitani, RSC Adv. 2014, 4, 45848-45855. (k) X. Tang, H. Chen, L. Hu, W. Hao, Y. Sun, X. Zeng, L. Lin, S. Liu, Appl. Catal. B. Env. 2014, 147, 827-834. (l) B. Cai, X.C. Zhou, Y.C. Miao, J.Y. Luo, H. Pan, Y.B. Huang, ACS Sustain. Chem. Eng. 2017, 5, 1322-1331. (m) Z. Yang, Y.B. Huang, Q.X. Guo, Y. Fu, Chem. Commun. 2013, 49, 5328-5330. (n) J. A. Melero, G. Morales, J. Iglesias, M. Paniagua, C. Lopez-Aguado, K. Wilson, A. Osatiashtiani, Green Chem. 2017, 19, 5114-5121.

8 P. Kumar, A.K. Singh, R. Pandey, P.Z. Li, S.K. Singh, Q. Xu, D.S. Pandey, J. Organomet. Chem. 2010, 695, 2205-2212.

9 (a) S. Wang, V. Dorcet, T. Roisnel, C. Bruneau, C. Fischmeister, Organometallics 2017, 36, 708-713. (b) G. Amenuvor, B.C.E. Makhubela, J. Darkwa, ACS Sust. Chem. Eng. 2016, 4, 6010-6018.

10 (a) J. Deng, Y. Wang, T. Pan, Q. Xu, Q.Z. Guo, Y. Fu, ChemSusChem 2013, 6, 1163-1167. (b) S. Wang, H. Huang, V. Dorcet, T. Roisnel, C. Bruneau, C. Fischmeister, Organometallics 2017, 36, 3152-3162. (c) W.-P. Wu, Y.-J. Xu, S.-W. Chang, J. Deng, Y. Fu, ChemCatChem 2016, 8, 3375-3380.

11 C. Ortiz-Cervantes, M. Flores-Alamo, J.J. García, ACS Catal. 2015, 5, 1424-1431.

12 Recent references include: a) J. M. Stubbs, R. J. Hazlehurst, P. D. Boyle, J. M. Blacquiere, Organometallics 2017, 36, 1692−1698. (b) M. Simonetti, M.; Perry,; Cambeiro, X. C.; Hernàndez, F.-J.; Arokianathar, J. N.; Larrosa, I., J. Am. Chem. Soc. 2016, 138, 3596−3606. (c) D. Zell, S. Warratz, D. Gelman, S. J. Garden, L. Ackermann, Chem. Eur. J. 2016, 22, 1248-1252. (d) J. Malineni, H. Keul, M. Möller, Dalton Trans. 2015, 44, 17409-17414.

13 (a) L. Zeng, P. Gupta, Y. Chen, E. Wang, L. Ji, H. Chao, Z.-S. Chen, Chem. Soc. Rev. 2017, 46, 5771-5804. (b) P. Zhang, P. J. Sadler, J. Organomet. Chem. 2017, 839, 5-14. (c) A. A. Nazarov, C. G. Hartinger, P. J. Dyson, J. Organomet. Chem. 2014, 751, 751, 251-260. (d) A. K. Singh, D. S. Pandey, Q. Xu, P. Braunstein, Coord. Chem. Rev. 2014, 270–271, 31–56.

14 Selected references are: a) K. M. Steward, E. C. Gentry, J. S. Johnson, J. Am. Chem. Soc. 2012, 134, 7329-7332. (b) J. Canivet, G. Süss-Fink, Green Chem. 2009, 9, 391-397. (c) D. Sterk, M. Stephan, B. Mohar, Org.

View Article Online
DOI: 10.1039/C8NJ03569E

Lett. 2006, 8, 5935-5938. (d) A. B. Chaplin, P. J. Dyson, Organometallics 2007, 26, 4357-4360. (e) T. Marimuthu, H. B. Friedrich, ChemCatChem 2012, 4, 2090-2095.

15 R. Noyori, Angew. Chem. Int. Ed. 2002, 41, 2008-2022. (b) B. Vilhanová, J. Vaclavík, P. Šot, J. Pecháček, J. Zápal, R. Pažout, J. Maixner, M. Kuzma, P. Kačer, Chem. Commun. 2016, 52, 362-365.

16 A. S. Amarasekara, M. A. Hasan, Catal. Commun. 2015, 60, 5-7.

17 (a) L. Biancalana, I. Abdalghani, F. Chiellini, S. Zacchini, G. Pampaloni, M. Crucianelli, F. Marchetti, Eur J. Inorg. Chem. 2018, 3041-3057. (b) S. Lutsenko, C. Moberg, Tetrahedron: Asymmetry 2001, 12, 2529-2532.

18 (a) N. E. Leadbeater, Adv. Pol. Sci. 2016, 274, 1-44. (b) A. K. Rathi, M. B. Gawande, R. Zboril, R. S. Varma, Coord. Chem. Rev. 2015, 291, 68-94. (c) N. E. Leadbeater, Ed. by P. Knochel, G. A. Molander, Compr. Org. Synth. (2nd Edition), 9, 234-286. (d) M. B. Gawande, S. N. Shelke, R. Zboril, R. S. Varma, Acc. Chem. Res. 2014, 47, 1338-1348. (e) A.M. Raspolli Galletti, C. Antonetti, M. Bertoldo, F. Piccinelli, Appl. Catal. A: Gen. 2013, 468, 95-101. (f) C. Antonetti, M. Melloni, D. Licursi, S. Fulignati, E. Ribechini, S. Rivas, J.C. Parajó, F. Cavani, A.M. Raspolli Galletti, Appl. Catal. B: Env. 2017, 206, 364-377.

19 (a) J. M. Kliegman, R. K. Barnes, Tetrahedron 1970, 26, 2555-2560. (b) I. E. Buys, S. Elgafi, L. D. Field, T. W. Hambley, B. A. Messerle, Inorg. Chem. 1994, 33, 1539-1542.

20 L. Biancalana, L. K. Batchelor, T. Funaioli, S. Zacchini, G. Pampaloni, P. J. Dyson, F. Marchetti, Inorg. Chem. 2018, 57, 6669−6685.

21 a) K. Yang, R. J. Lachicotte, R. Eisenberg, Organometallics 1997, 16, 5234-5243. (b) D. Dange, S. L. Choong, C. Schenk, A. Stasch, C. Jones, Dalton Trans. 2012, 41, 9304-9315. (c) P. Saha, D. Samanta, P. Ghosh, New J. Chem. 2017, 41, 1149-1159.

22 The choice of solvent is crucial to the success of each reaction. In the cases of [**1**]NO_3 and [**5**]NO_3, performing the reaction in methanol (rather than acetonitrile) resulted in the formation of a mixture of products.

23 The choice of solvent is crucial to the success of each reaction. In the cases of [**1**]NO_3 and [**5**]NO_3, performing the reaction in methanol (rather than acetonitrile) resulted in the formation of a mixture of products.

24 a) H. T. Dieck, W. Kollvitz, I. Kleinwachter, Organometallics 1986, 5, 1449-1457. (b) G. Ciancaleoni, C. Zuccaccia, D. Zuccaccia, A. Macchioni, Organometallics 2007, 26, 3624-3626.

25 (a) D. Zuccaccia, S. Sabatini, G. Bellachioma, G. Cardaci, E. Clot, A. Macchioni, Inorg. Chem. 2003, 42, 5465-5467. (b) D. Zuccaccia, G. Bellachioma, G. Cardaci, G. Ciancaleoni, C. Zuccaccia, E. Clot, A. Macchioni, Organometallics 2007, 26, 3930-3946.

26 (a) R. E. Morris, R. E. Aird, P. d. S. Murdoch, H. Chen, J. Cummings, N. D. Hughes, S. Parsons, A. Parkin, G. Boyd, D. I. Jodrell, P. J. Sadler, J. Med. Chem. 2001, 44, 3616-3621. (b) S. B. Jensen, S. J. Rodger, M. D. Spicer, J. Organomet. Chem. 1998, 556, 151–158. (c) F. B. McCormick, D. D. Cox, W. B. Gleason, Organometallics 1993, 12, 610-612.

View Article Online
DOI: 10.1039/C8NJ03569E

27 (a) H. T. Dieck, I. W. Renk, Chem. Ber. 1971, 104, 92-102. (b) N. Bartalucci, M. Bortoluzzi, G. Pampaloni, C. Pinzino, S. Zacchini, F. Marchetti, Dalton Trans. 2018, 47, 3346–3355. (c) N. Bartalucci, M. Bortoluzzi, S. Zacchini, G. Pampaloni, F. Marchetti, New J. Chem. 2018, 42, 8503-8511.

28 (a) D. Braga, Chem. Rev. 1992, 92, 633–665. (b) T. A. Albright, Acc. Chem. Res. 1982, 15, 149–155.

29 Selected references: a) F. Martinez-Peña, A. M. Pizarro, Chem. Eur. J. 2017, 23, 16231-16241. (b) C. Guan, D.-D. Zhang, Y. Pan, M. Iguchi, M. J. Ajitha, J. Hu, H. Li, C. Yao, M.-H. Huang, S. Min, J. Zheng, Y. Himeda, H. Kawanami, K.-W. Huang, Inorg. Chem. 2017, 56, 438−445. (c) J. Palmucci, F. Marchetti, R. Pettinari, C. Pettinari, R. Scopelliti, T. Riedel, B. Therrien, A. Galindo, P. J. Dyson, Inorg. Chem. 2016, 55, 11770−11781. (d) M. Kubanik, H. Holtkamp, T. Söhnel, S. M. F. Jamieson, C. G. Hartinger, Organometallics 2015, 34, 5658−5668. (e) C. M. Clavel, E. Păunescu, P. Nowak-Sliwinska, A. W. Griffioen, R. Scopelliti, P. J. Dyson, J. Med. Chem. 2015, 58, 3356−3365.

30 a) M. Yamakawa, H. Ito, R. Noyori, J. Am. Chem. Soc. 2000, 122, 1466-1478. (b) P. A. Dub, J. C. Gordon, ACS Catal. 2017, 7, 6635−6655. (c) P. A. Dub, J. C. Gordon, Dalton Trans. 2016, 45, 6756-6781. (d) J. S. M. Samec, J. E. Bäckvall, P. G. Andersson, P. Brandt, Chem. Soc. Rev. 2006, 35, 237–248.

31 Selected recent references: (a) J. M. Gichumbi, H. B. Friedrich, B. J. Omondi, Mol. Catal. A: Chem. 2016, 416, 29–38. (b) N. Meriç, C. Kayan, N. Gürbüz, M. Karakaplan, N. E. Binbay, M. Aydemir, Tetrahedron: Asymm. 2017, 28, 1739–1749. (c) Y.-H. Chang, W.-J. Leu, A. Datta, H.-C. Hsiao, C.-H. Lin, J.-H. Guh, J.-H. Huang, Dalton Trans. 2015, 44, 16107-16118. (d) R. Aznar, A. Grabulosa, A. Mannu, G. Muller, D. Sainz, V. Moreno, M. Font-Bardia, T. Calvet, J. Lorenzo, Organometallics 2013, 32, 2344-2362.

32 (a) C. Kerner, J. Lang, M. Gaffga, F. S. Menges, Y. Sun, G. Niedner-Schatteburg, W. R. Thiel, ChemPlusChem 2017, 82, 212-224. (b) F. Sepulveda, M. C. Carrion, A. D. Phillips, F. A. Jalon, P. J. Dyson, B. R. Manzano, Eur. J. Inorg. Chem. 2017, 630-638. (c) J. DePasquale, M. Kumar, M. Zeller, E. T. Papish, Organometallics 2013, 32, 966-979. (d) M. C. Carrión, F. Sepúlveda, F. A. Jalón, B. R. Manzano, Organometallics 2009, 28, 3822-3833.

33 H. Li, Z. Fang, S. Yang, ChemPlusChem 2016, 81, 135-142.

34 (a) W. Li, J. Xie, H. Lin, Q. Zhou, Green Chem. 2012, 14, 2388-2390. (b) A. Kanchanadevi, R. Ramesh, D. Semeril, J. Organometallic Chem. 2016, 808, 68-77.

35 R. S. Assary, L. A. Curtiss, Chem. Phys. Lett. 2012, 541, 21-26.

36 See Supporting Information (Figures S25, S31, S32, and page S39). When to run 5, after 30 min of reaction time (Table 3, reached conversion 51%), 5 mmol of fresh EL were added, no further reaction advancement was ascertained.

37 M. A. Bennett, A. K. Smith, J. Chem. Soc., Dalton Trans. 1974, 233-241.

38 G. R. Fulmer, A. J. M. Miller, N. H. Sherden, H. E. Gottlieb, A. Nudelman, B. M. Stoltz, J. E. Bercaw, K. I. Goldberg, Organometallics 2010, 29, 2176–2179.

39 W. Willker, D. Leibfritz, R. Kerssebaum, W. Bermel, Magn. Reson. Chem. 1993, 31, 287-292.

View Article Online
DOI: 10.1039/C8NJ03569E

40 F. Menges, "Spectragryph - optical spectroscopy software", Version 1.2.5, @ 2016-2017, http://www.effemm2.de/spectragryph.

41 (a) A. Jutand, Eur. J. Inorg. Chem. 2003, 2017-2040. b) W. J. Geary, Coord. Chem. Rev. 1971, 7, 81-122.

42 G. M. Sheldrick, SADABS-2008/1 - Bruker AXS Area Detector Scaling and Absorption Correction, Bruker AXS: Madison, Wisconsin, USA, 2008.

43 G. M. Shekdrick, Acta Cryst. 2015, C71, 3-8.

View Article Online
DOI: 10.1039/C8NJ03569E

Ruthenium *p*-Cymene Complexes with α-Diimine Ligands as Catalytic Precursors for the Transfer Hydrogenation of Ethyl Levulinate to γ-Valerolactone

Lorenzo Biancalana, Sara Fulignati, Claudia Antonetti, Stefano Zacchini, Giacomo Provinciali, Guido Pampaloni, Anna Maria Raspolli Galletti and Fabio Marchetti

Cationic Ru(II) arene complexes with α-diimine ligands were investigated as catalytic precursors in the transfer hydrogenation of ethyl levulinate to γ-valerolactone from isopropanol, under MW irradiation. Variable reaction conditions are discussed, including the critical choice of the counter anion.